Electronic Supplementary Material (ESI) for Lab on a Chip.

Automated Raman based cell sorting with 3D microfluidics

Yingkai Lyu,[a,b] Xiaofei Yuan,[a,c] Andrew Glidle,[a] Yuchen Fu,[a] Hitoshi Furusho,[d] Tianxin Yang,*[b] and Huabing Yin *[a]

[a] Division of Biomedical Engineering, School of Engineering, University of Glasgow, Glasgow G12 8LT, UK.

[b] Key Laboratory of the Ministry of Education on Optoelectronic Information Technology, School of Precision Instrument and Optoelectronics Engineering, Tianjin University, Tianjin 300072, China.

[c] School of Environmental Science and Engineering, Southern University of Science and Technology, Shenzhen, Guangdong, 518055, China.

[d] Nissan Chemical Ltd., 5-1, Nihonbashi 2-Chome, Chuo-ku, Tokyo 103-6119, Japan.

Corresponding authors: tyang@tju.edu.cn and huabing.yin@glasgow.ac.uk

Supporting information content

Supporting information S1. Device design, fabrication and assembly.

Supporting information S2. Theoretical evaluation of accuracy and purity of sorted samples.

Supplementary Figure S1. COMSOL CFD simulation of 3D flow focusing.

Supplementary Figure S2. 3D printed chamber and assembling of two modules.

Supplementary Figure S3. Flow charts of the sorting process and the control program.

Supplementary Figure S4. Experimental setup.

Supplementary Figure S5. Flow focus in the detection chamber.

Supplementary Figure S6. Time-lapse images of switching events at sorting module.

Supplementary Figure S7. Simulation of sorting accuracy and purity.

Supplementary Figure S8. In-line collection and analysis of cell purity.

Supplementary Table S1. Sorting performance over 8 hours.

Supplementary Video S1. Flow focus of 3 μm demonstrated by fluorescent beads.

Supplementary Video S2. Automated, Raman activated single cell sorting. Target and non-target cells are directed to alternate outlets with 75 ms switch time.

33

Supporting information S1:

Device design, fabrication and assembly

Overview

The device consists of a 3D printed detection unit and a PDMS based sorting unit. The 3D printed focussing and detection module was fabricated with an Object30 Prime printer using Veroclear and soluble support SUP706. The sorting module was fabricated using a moulded PDMS (Polydimethylsiloxane) channel structure bonded to a glass coverslip to enable high speed video acquisition of fast flowing cells at the sorting junction (note, the optical transparency of the in-house printed device is not sufficient for this purpose). The current device designs have to consider the constraints in 3D printing (detailed below); however, it is envisaged a fully 3D printed device will be achieved with a high-resolution 3D printer in the near future.

Design considerations for the 3D printed detection chamber

The main printing constraint was imposed by the diameters of the smallest hole for the inlet and outlet sample and sheath flow streams, which could be made reliably using the Objet30 and the clear resin. This was found to be ~100 μm.

Initial COMSOL simulations and experiments showed that for a sample detection chamber of ~1 mm x 1 mm, the diameter of the inlet sample capillary should be <50 μm in order to obtain a focussed flow profile of ~10 μm at the laser focus which extended over a length of 100-200 μm (Supplementary Figure S1). Thus, the most convenient way to achieve this using a 3D printed device, was to use a 40 μm internal diameter fused silica capillary inserted into a larger hole in the 3D printed detection module.

Having set the size of the sample inlet capillary, the capillaries delivering the four inlet sheath flows were then placed as close as possible, in a radial fashion around this central capillary, forming a pattern similar to the 5 dots on the face of a dice (Supplementary Figure S2A). To convey the larger flow rates required to achieve the desired sheath flow focussing, flexible 150 μm internal diameter PEEK capillaries (Part. No.: TPK.106-10M) inserted into the 3D printed part were used. The microfluidic design aspect of the detection chamber was

completed by arranging for the outlet sheath and sample flows to exit through capillaries that were placed in a mirror image of the inlet ones (Figure 1 in the main text).

The final feature in the 3D printed detection chamber is the insertion of a 105 μm core multimode fibre into a hole, centrally placed into the side of the chamber, oriented perpendicular to the sample inlet-outlet streams (Supplementary Figure S2A, cross-section). This fibre is inserted so that it points towards the mid-point (in x, y and z) of the detection chamber, where the flow focus and laser focus are co-incident.

Design considerations for the sorting channel network

The sorting channel network comprises 150 μm wide channels for the fluid flow with two blind channels for the optical fibres of the beam-break sensor (Figure 1 of the main text). To achieve the fastest switching rates and prevent blockage, it is desirable for the fluid to flow in these channels at high speeds. Thus, a 50 μm high SU-8 layer was used to define the microfluidic network. However, the diameter of the optical fibres, fused silica capillary (from the detection chamber), and the PEEK capillaries used to convey the collected sample away from the device were significantly larger. Thus, when fabricating the SU-8 mould used to define the PDMS replica, after exposure and post-exposure baking of the first pattern, a second layer of SU-8 was spun on top of the first layer. The two exposed layers were then developed at the same time to yield a terraced mould.

Connecting the subunits.

To realise a complete cell sorting device, the two subunits were connected via a short (~10 mm) 50 μm internal diameter fused silica capillary (Supplementary Figure S2B). The fused silica capillary was sealed in place using silicone rubber RTV3140.

Supporting information 2:

Theoretical evaluation of accuracy and purity of sorted samples

Three elements in the sorting device contribute to the efficiency of sorting and the purity of the sorted sample: 1) detection of a target cell in the detection chamber; 2) detection of a detected target cell when it passes optical sensor 2 in the sorting channel network; and 3) switching of a detected target cell into the collection channel by the pressure unit. All three of these factors are influenced by both the speed of the cells and the throughput. For example,

98 if the laser spot is defocussed to 10 μm wide at the flow focus point, then for cells travelling
99 at 1 mm/s and a sCMOS camera readout time of 10 ms, very few target cells will be missed.
100 (Time taken to pass through the laser spot = 10 μm / (1 mm/s) = 10 ms).
101
102 Overlaid on the above instrumental and program factors, the measured accuracy and purity of
103 a sorted sample are also influenced by the relative concentrations of target and non-target
104 cells in the initial sample. In general, the factors described below have been well discussed in
105 the evaluation of FACS systems and thus only an outline relating to how these are applied to
106 this system are described here.
107
108 **Accuracy of sorting detected cells**
109 The accuracy of detecting a target cell at optical sensor 2 in the sorting unit is related to the
110 variation in transit time from the laser spot to the sensor. As shown in Figure 5B, this
111 variation is close to a normal distribution with a standard deviation of 5-10%. Based on a
112 normal distribution assumption, if the software controlling the sensor is set to read data in a
113 time interval of +/- 2σ of the expected time, then target cells could be detected with 95%
114 accuracy if they are sparsely separated from other cells in the sample flow stream. However,
115 Poisson statistics predict that in a sample stream with a high cell density, flowing at a high
116 throughput rate, there will inevitably be occasions when a non-target cell arrives at the beam-
117 break sensor before the target one. For example, if the throughput is 10 cells/s and the time
118 interval during which the sensor is being monitored is 46 ms (as in Figure 5B), then the
119 probability of two cells being present during this interval is ~19%. This falls to 10% if the
120 throughput falls to 5 cells/s or the transit time reduces to ~100 ms.
121
122 In terms of influencing the accuracy of sorting the target cells, the non-target cell will pass
123 before the target one on 50% of the times when two cells are within this +/- 2σ interval.
124 These occasions will lead to an 'early' trigger of the sorting channel pressure switching
125 procedure. Thus for the conditions of Figure 5, the predicted sorting accuracy is ~90% (90%
126 = 95% - 10%/2), as found in the data of Figure 6A.
127
128 These values were confirmed by Matlab modelling of a randomly distributed train of target
129 and non-target cells flowing at various flow rates and having a distribution of detector to
130 optical sensor 2 transit times (Supplementary Figure S7A). This modelling predicted that the

most effective way of improving the accuracy of sorting would be to improve the prediction of the transit time for a particular target cell, or reduce the spread in transit times, as expected.

Other methods to improve the accuracy (e.g. to 98%) can be achieved by reducing the cell throughput. Alternatively, the scattering signal provided by the optical fibre in the detection chamber could be used to provide information about when non-target cells were likely to arrive at the beam-break sensor, thereby eliminating the occasions on which false triggering occurred.

Purity of sorted sample

As indicated in the preceding section, the purity of the sorted sample can be reduced if a non-target cell arrives at optical sensor 2 in advance of the designated target one. However, for the conditions of Figure 6B, this leads to a 5% reduction in purity at worst. The principle factors reducing the purity are the time interval for which the pressure switch is applied, the cell throughput and the relative concentration of target and non-target cells in the sample stream. Again, Poisson statistics apply, and if the sorting channel flow is diverted to the collection channel for, say 75 ms, and the throughput is 156 cells/min (as in Figure 6B), then for, at most, ~15% of the switching events, a non-target cell will be switched with the target one. The probability of this 'non-target' cell (and so decreasing the purity), is proportional to the relative concentrations of target and non-target cells in the initial sample. Thus, if the initial sample concentration comprises 21.2% target cells (as in Figure 6B), then for ~12% of the switches, an undesirable cell will be included in the sorted target cell stream (12% = (0.85 (fraction of correct target switches) + 0.212 x 0.15 (additional target cells in double cell switches) + 0.15 (designated target cell in double switches))/(0.85 (correct target switches) + 2 x 0.15 (no. of double switches)). Adding to this the reduction in purity due to the beam-break sensor triggering on a non-target cell, leads to a purity of 75% - 85% for the conditions of Figure 6B.

Again, the above estimates based on statistical theory are consistent with Matlab modelling of a random train of cells passing through the system (Supplementary Figure S7B). Both the theory and model indicate that improvements of this purity can be readily made by reducing the throughput and reducing the switching time.

Supplementary Figures:

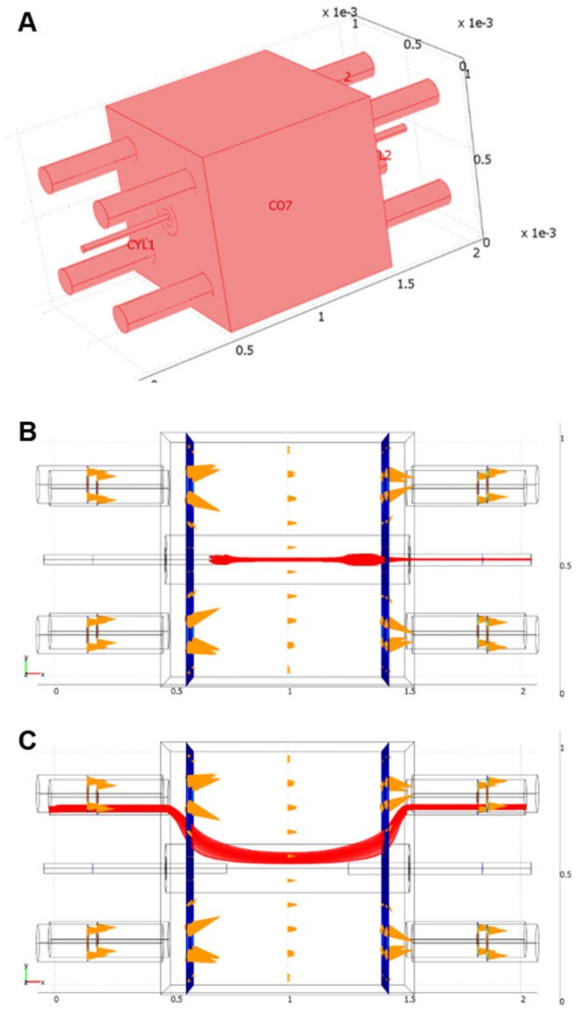

Supplementary Figure S1: COMSOL CFD simulation of 3D flow focusing. (A) A schematic of the flow channels, with four inlet sheath flow channels surrounding a central sample inlet channel, denoted CYL1. These flow into a detection chamber (CO7), with the sheath flow and sample solutions exiting the detection chamber via a set of five channels that mirror those on the inlet side of the chamber. (B) Top view of panel (A), showing the focussed sample flow more clearly, with sample and sheath flow parameters adjusted to realise a focus flow cross section of 10 µm, and a sample velocity of 1 mm/s. (C) A second top view of panel (A), showing how streamlines from the sheath flow effectively focus the sample flow to achieve the desired cross section (streamlines from one sheath flow stream only are shown, for clarity).

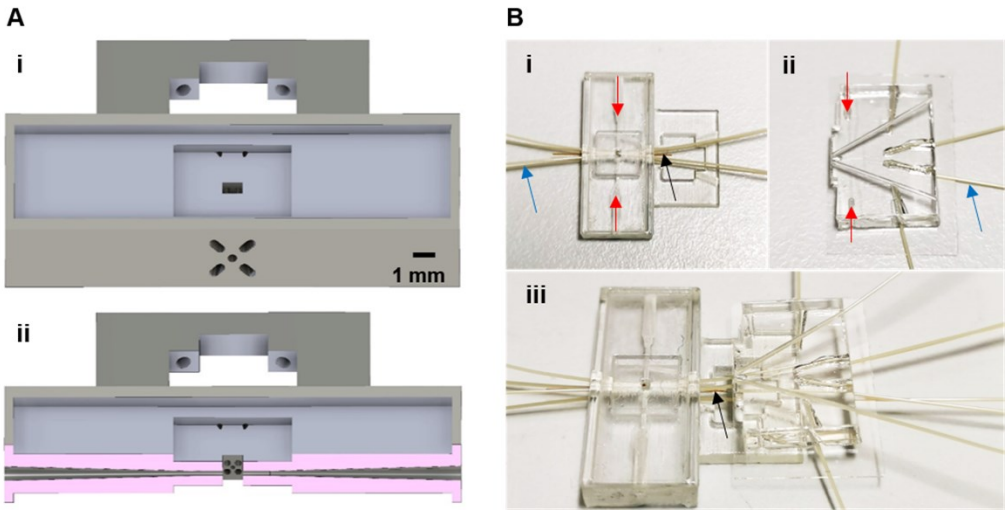

Supplementary Figure S2: (A) i- 3D overview of the 3D printed module. The pattern of the holes is mirrored on the opposite side of the device. The central square (~1 mm) hole is for the detection chamber. The rear part of the device serves to hold the separately fabricated PDMS sorting module. ii- A cross section view of the detection chamber, showing the holes (indicated by arrow) are used to insert the optical fibres. (B) i- 3D printed detection chamber connected with sheath flow capillary tubing (blue arrow, ID=150 µm) and fused silica capillary tubing (black arrow, ID=50 µm). Red arrows indicate the channels for fibres; ii- PDMS module connected with sorting capillary tubing (blue arrow). Red arrows indicate the channels for fibres; iii- Assembled modules before glueing. Black arrow indicates the fused silica capillary tubing, which connects the detection chamber and sorting module.

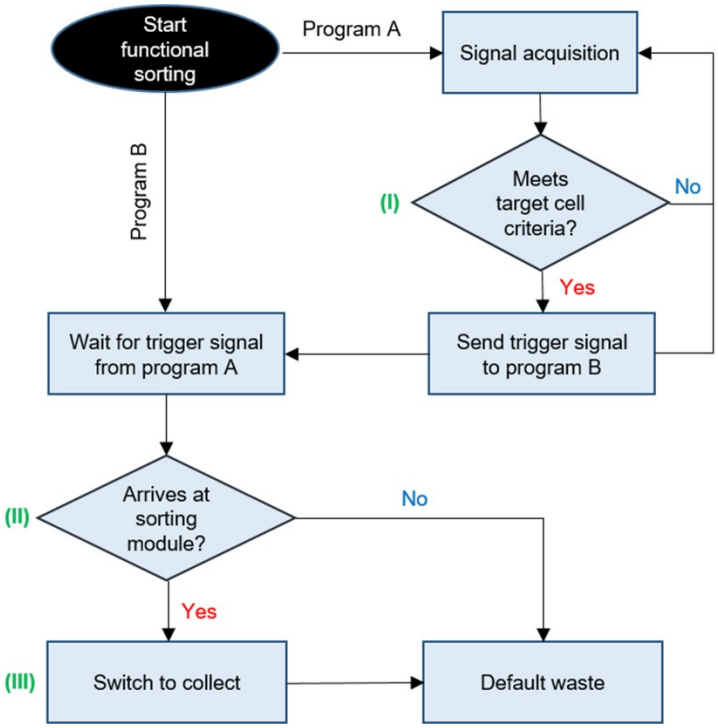

Supplementary Figure S3: (B) A flow chart of the control program. Program A controls the camera and Program B controls the pressure switch.

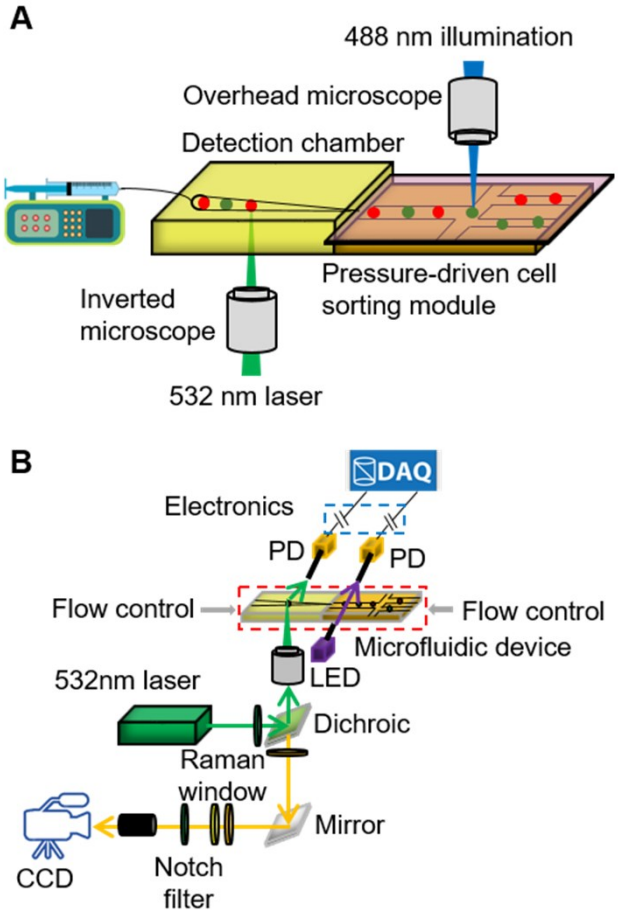

Supplementary Figure S4: (A) Overview of the platform. (B) Schematic of the experimental setup. Red dotted rectangular is a representative of the microfluidic device. Electronics include I/V converter, amplifier and wave filter. Raman window involves single-band bandpass filters of 576/10 nm and 609/62 nm. DAQ: data acquisition. LED: light-emitting diode. CCD: charge-coupled device.

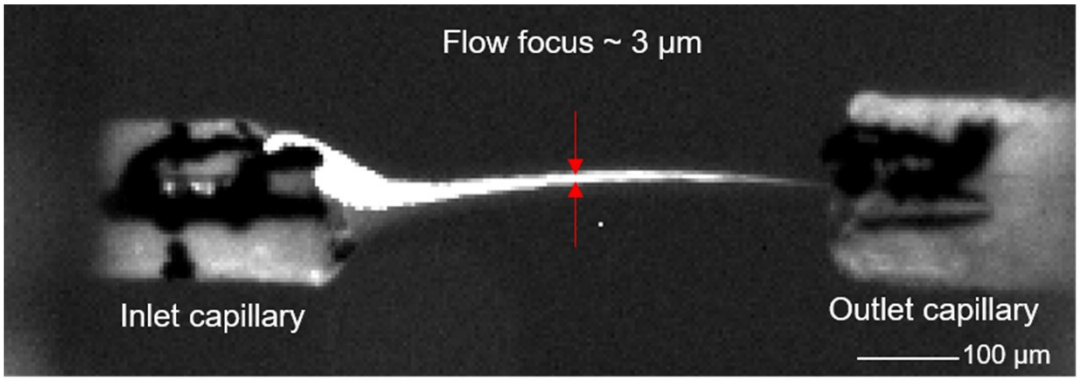

Supplementary Figure S5: Flow focus in the detection chamber. The figure is constructed by overlaying multiple frames each containing individual cells, from the Supplementary Video S1 (the fluorescence signals from these cells form the white flow path shown as the focussed flow). The less bright features at either end of this white streak correspond to the background fluorescence of the inlet and outlet capillaries (enhanced here to aid visibility).

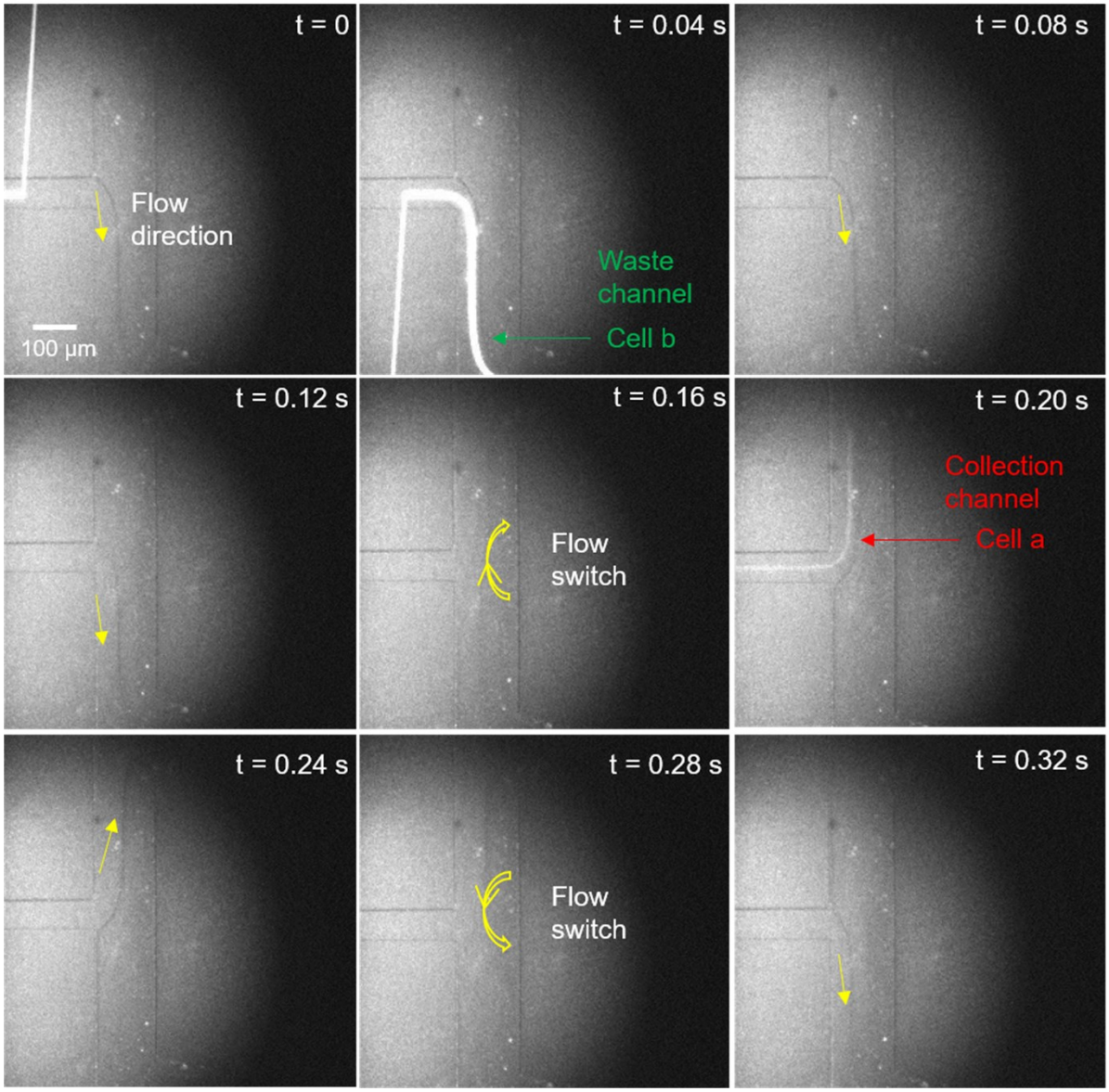

Supplementary Figure S6: Time-lapse images showing that the sample flow was switched to direct a target "cell a" and a non-target "cell b" to the appropriate channels. The yellow arrows indicate the flow direction. Note, due to the 488 nm illumination in the overhead microscope, the Calcein AM labelled non-target cell appeared brighter than the targeted cell (labelled with CellTrace yellow). Switch time=75 ms, Supplementary Video S2. The bright line in the first two subfigures are the ghost images from CCD.

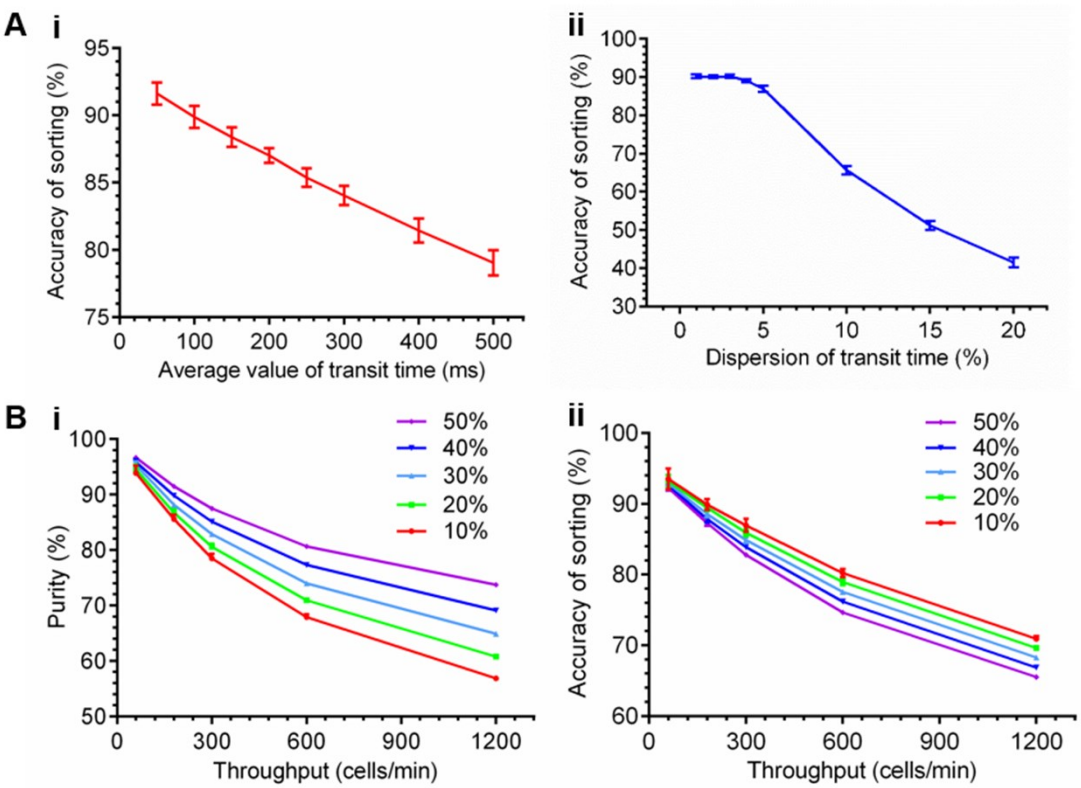

Supplementary Figure S7: (A) Simulation of the accuracy of sorting as a function of (i) the average transit time from the detection point to optical sensor 2 (based on 5% dispersion) and (ii) the dispersion of transit time (based on 200 ms average transit time). The initial target cell percentage: 10%; throughput: 300 cells/min. (B) Simulation of the effect of throughput on (i) purity and (ii) accuracy of sorting at different initial target concentrations (i.e. from 10% to 50%). Average value and dispersion of transit time are 200 ms and 5%, respectively.

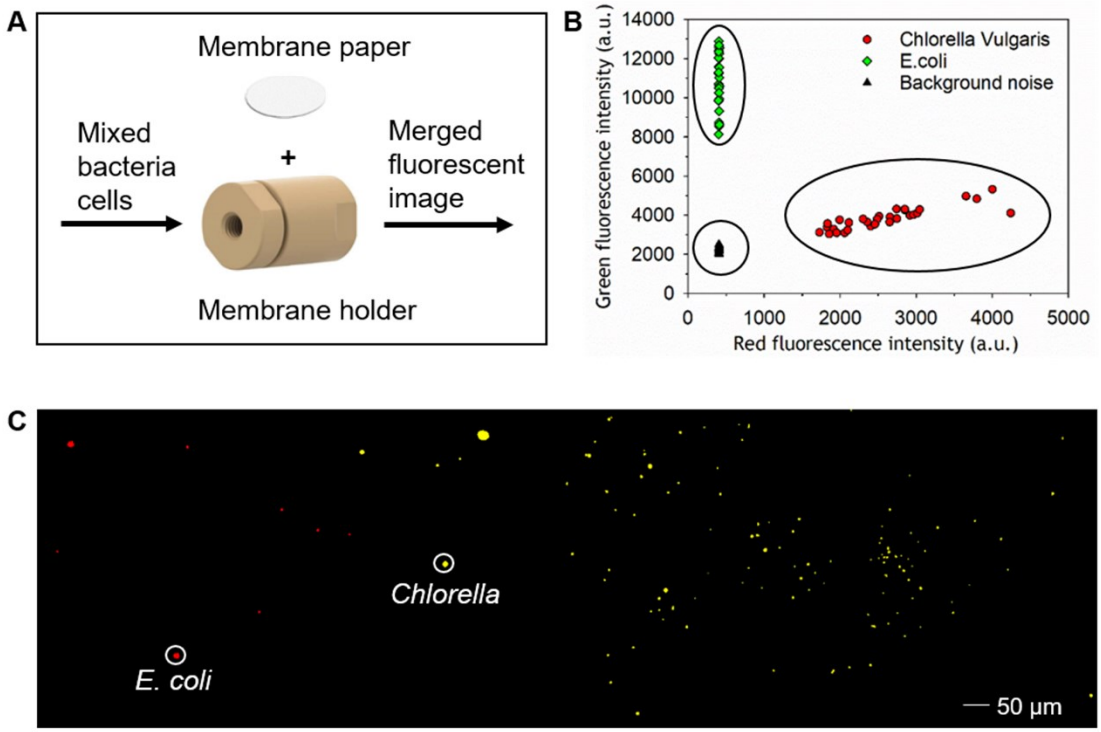

Supplementary Figure S8: (A) Diagram of the membrane filter for online collection of sorted cells. The filter was created by placing a membrane paper into a holder. (B) Clustering analysis of the red and green fluorescence intensity of *Chlorella Vulgaris* and *E. coli* cells on a membrane paper shows clear separation between them. Rhodamine and FITC filters were used to image cells on the membrane filter. (C) Composite fluorescence image of a representative area of the filter paper. Pseudo colour: yellow- *Chlorella Vulgaris* and red - *E. coli*.

Supplementary Table 1: Sorting performance over 8 hours [a]

Time (h)		1	2	3	4	5	6	7	8	Total
Collection [b]	Targets	36	13	14	20	19	18	31	16	167
	Non-targets	10	4	4	7	5	6	10	5	51
Waste [b]	Targets	6	3	2	5	4	5	3	2	30
	Non-targets	194	220	208	234	250	261	223	236	1826
Total number		246	240	228	266	278	290	267	259	2074
Purity (%)		78.3	76.5	77.8	74.1	79.2	75.0	75.6	76.2	76.6±1.6
Accuracy of sorting (%)		85.7	81.3	87.5	80.0	82.6	78.3	91.2	88.9	84.4±4.3

[a] Automated sorting operation for > 8 hours. 60-second video recordings were taken hourly to evaluate the sorting performance. The initial target bead percentage was 10% and the average throughput was 260 beads/min.

[b] The number of target beads and the number of non-target beads in the collection or in the waste.